Critical Time Course of Right Frontoparietal Involvement in Mental Number Space

Elena Rusconi[1,2,3], Martynas Dervinis[4], Frederick Verbruggen[4,5], and Christopher D. Chambers[4]

Abstract

■ Neuropsychological, neurophysiological, and neuroimaging studies suggest that right frontoparietal circuits may be necessary for the processing of mental number space, also known as the mental number line (MNL). Here we sought to specify the critical time course of three nodes that have previously been related to MNL processing: right posterior parietal cortex (rPPC), right FEF (rFEF), and right inferior frontal gyrus (rIFG). The effects of single-pulse TMS delivered at 120% distance-adjusted individual motor threshold were investigated in 21 participants, within a window of 0–400 msec (sampling interval = 33 msec) from the onset of a central digit (1–9, 5 excluded). Pulses were delivered in a random order and with equal probability at each time point, intermixed with noTMS trials. To analyze whether and when TMS interfered with MNL processing, we fitted bimodal Gaussian functions to the observed data and measured effects on changes in the Spatial–Numerical Association of Response Codes (SNARC) effect (i.e., an advantage for left- over right-key responses to small numbers and right- over left-key responses to large numbers) and in overall performance efficiency. We found that, during magnitude judgment with unimanual key-press responses, TMS reduced the SNARC effect in the earlier period of the fitted functions (~25–60 msec) when delivered over rFEF (small and large numbers) and rIFG (small numbers); TMS further reduced the SNARC effect for small numbers in a later period when delivered to rFEF (~200 msec). In contrast, TMS of rPPC did not interfere with the SNARC effect but generally reduced performance for small numbers and enhanced it for large numbers, thus producing a pattern reminiscent of "neglect" in mental number space. Our results confirm the causal role of an intact right frontoparietal network in the processing of mental number space. They also indicate that rPPC is specifically tied to explicit number magnitude processing and that rFEF and rIFG contribute to interfacing mental visuospatial codes with lateralized response codes. Overall, our findings suggest that both ventral and dorsal frontoparietal circuits are causally involved and functionally connected in the mapping of numbers to space. ■

INTRODUCTION

Studies on number processing have begun to delineate core cognitive and neural aspects of mathematics. Although we are still far from formulating a model of the most complex human mathematical skills, a coherent picture is emerging of its evolutionary precursors and elementary components. For example, it is generally accepted that core numerical abilities rest on abstract numerosity or quantity representations, which require an intact and fully functional bilateral horizontal intraparietal sulcus (e.g., Butterworth, 2010; Ansari, 2008; Dehaene, Piazza, Pinel, & Cohen, 2003). In both humans and nonhuman primates, such posterior parietal neural populations activate consistently during quantity processing. These populations appear to be intermingled with—but distinct from—those encoding object size and location and maintain a distinctive position relative to other posterior parietal areas that are primarily involved in sensory, motor, and attentional functions (e.g., Hubbard, Piazza, Pinel, & Dehaene, 2005; Simon, Mangin, Cohen, Le Bihan, & Dehaene, 2002, but see Walsh, 2003; see Nieder & Dehaene, 2009, for a comparative review). The neural correlates of number processing are, however, not restricted to bilateral intraparietal sulcus. In the monkey model of number processing, the parietal pathway quickly extracts nonsymbolic numerical attributes and feeds decisional processes occurring in pFC (Nieder & Miller, 2004).

In research on human participants, evidence is rapidly accumulating that when adults are explicitly engaged in number comparison tasks (often using Arabic symbols), additional areas are recruited—possibly via feed-forward projections from the intraparietal sulcus (see Sandrini, Umiltà, & Rusconi, 2011; Sandrini & Rusconi, 2009, for reviews). Such regions include extrastriate visual areas (e.g., Cattaneo, Silvanto, Battelli, & Pascual-Leone, 2009; Salillas-Pérez, Basso, Baldi, Semenza, & Vecchi, 2009); frontoparietal areas for spatial orienting, working memory, and response selection (e.g., Rusconi, Bueti, Walsh, & Butterworth, 2011; Cattaneo, Silvanto, Pascual-Leone, & Battelli, 2009; Rusconi, Turatto, & Umiltà, 2007); and representational or

[1]University of Parma, [2]University of Trento, [3]University College London, [4]Cardiff University, [5]University of Exeter

motor hand-related areas (e.g., Sato, Cattaneo, Rizzolatti, & Gallese, 2007; Rusconi, Walsh, & Butterworth, 2005). Thus, number processing in humans likely depends on a range of circuits that may not be primarily specialized for number processing and which overlap considerably with the frontoparietal network that has been implicated in the control of spatial attention (e.g., Corbetta, Patel, & Shulman, 2008; Corbetta & Shulman, 2002). With this study, we sought to investigate further the role of key substrates that have been traditionally linked to spatial attention but, according to recent evidence, may also contribute to number processing via related mental spatial representations.

A crucial behavioral marker of number space processing is the Spatial–Numerical Association of Response Codes (SNARC) effect, which in Western populations consists of a preferential mapping of small numbers on left responses and large numbers on right responses (Dehaene, Bossini, & Giraux, 1993; see Wood, Willmes, Nuerk, & Fischer, 2008, for a review). The SNARC effect has been traditionally interpreted as a by-product of a spatial representation of numbers, the "mental number line" (MNL; Dehaene et al., 1993; but see, e.g., Fitousi, Shaki, & Algom, 2009; Santens & Gevers, 2008, for alternative views). On the basis of the orderly distribution of small numbers in left hemispace and large numbers in right hemispace, one may predict that the spatial codes attached to number magnitude will influence response selection and generate a stimulus–response (S-R) compatibility effect (i.e., faster and more accurate responses when stimulus and response features overlap; Dehaene et al., 1993; Kornblum, Hasbroucq, & Osman, 1990). The SNARC effect can thus be operationally defined as the behavioral difference between incompatible trials (smaller numbers, right response and larger numbers, left response) and compatible trials (smaller numbers, left response and larger numbers, right response). It is also sometimes defined as the estimated slope of a linear regression model by assuming that the difference between left and right responses changes linearly with number magnitude (Lorch & Myers, 1990). The latter definition, however, is less appropriate than a categorical one in the context of a number magnitude judgment task (Gevers, Verguts, Reynvoet, Caessens, & Fias, 2006) and will not be adopted in this study.

At a neural level, the systems underlying the SNARC effect that link numbers, space, and response selection are unclear and may differ depending on task and response demands. It is generally assumed, however, that the numerous analogies found between numerical and visuospatial processing may be more than a coincidence or a useful heuristic and could actually point to shared neural substrates (see, e.g., Sandrini et al., 2011; Umiltà, Priftis, & Zorzi, 2009; de Hevia, Vallar, & Girelli, 2008; Fias & Fischer, 2005; Hubbard et al., 2005, for complementary reviews).

Recently, Rusconi et al. (2011) reported in a repetitive TMS (rTMS) study that two right frontal areas, right FEF (rFEF) and right inferior frontal gyrus (rIFG), play a causal role in the SNARC effect during magnitude but not parity judgment of the same numerical stimuli. Predictions about the involvement of right frontal areas in number processing follow from neurophysiological studies in monkeys, which show that pFC supports a temporary storage of number magnitude when doing so is task-relevant (Nieder & Miller, 2004); from neuropsychological studies in patients with hemineglect, suggesting that right pFC may play a causal role in number spatial representation (Doricchi, Guariglia, Gasparini, & Tomaiuolo, 2005); and from fMRI-based models of spatial attention, which postulate a tight functional coupling between ventral pFC in the right hemisphere and FEF (Corbetta et al., 2008). Here we sought to (a) extend Rusconi et al.'s (2011) findings in a different setting using a new set of participants and with a high-precision single-pulse TMS protocol, (b) specify the critical functional time course of the identified crucial nodes in a number magnitude judgment task, and (c) investigate both the contribution of right frontal areas and the contribution of right posterior parietal cortex (rPPC) within the same experimental protocol and the same participants.

Because rFEF and rIFG are functionally connected to rPPC (e.g., Corbetta & Shulman, 2002) and because previous rTMS and neuropsychological studies suggest a crucial role of the rPPC in explicit magnitude processing (e.g., Cattaneo, Silvanto, Pascual-Leone, et al., 2009; Göbel, Calabria, Farnè, & Rossetti, 2006; Oliveri et al., 2004; Zorzi, Priftis, & Umiltà, 2002), we also investigated parietal involvement to differentiate the functional contribution of anterior versus posterior components in this circuit. A single-pulse TMS protocol with multiple onset times was employed to track in real time the fate of number magnitude processing within the right frontoparietal network for space processing and its eventual mapping on to lateralized responses.

The SNARC effect occurs in the context of a speeded choice reaction task. One popular view and the one we adopt here maintains that number magnitude processing makes use of an MNL (Dehaene et al., 1993). Number magnitude would thus be associated with a mental spatial layout that, because of task instructions and the range of target numbers used here, is centered on the explicit numerical reference (in this case, the number 5). Although all targets appear centrally and no overt saccades are required, spatial attention may need to be engaged to identify, select, and compare targets to the reference along the MNL before selecting an appropriate lateralized response. Such operations would be crucial to confer a spatial code to numbers, which may conflict or facilitate with lateralized response alternatives (see also Rusconi et al., 2007). The operations requested to locate, select, and compare numbers along the MNL may require the same (or analogous) neural operations as the location, selection, and comparison of visual targets in physical space.

It is well established that visual task performance can be modulated by TMS over the primary visual cortex and other early visual areas (e.g., motor threshold) during separate time windows (typically, two time windows in very simple visual tasks; see, e.g., Stevens, McGraw, Ledgeway, & Schluppeck, 2009; Juan, Campana, & Walsh, 2004, for a review of earlier studies). However, this biphasic involvement is by no means an exclusive property of classical sensory areas: A typical finding in studies of both human and nonhuman primates is a biphasic temporal profile in the same frontoparietal areas during a single task involving overt/covert attention and sensorimotor transformations (see, e.g., Barash, 2003, for a review of studies in the monkey; see Umarova et al., 2010; Chambers, Payne, Stokes, & Mattingley, 2004, for relevant studies on humans). Downstream associative regions, such as the angular gyrus, have been shown to contribute to visuospatial orienting tasks at discrete timepoints (see, e.g., Chambers et al., 2004), and stimulation of prefrontal regions, such as the FEF, may elicit a similar biphasic signature (see, e.g., Juan et al., 2008).

Biphasic involvement of a brain region can occur because different and/or partially overlapping neuronal populations in the same region subserve different functions (e.g., visual analysis and motor response preparation, Juan et al., 2008; transient vs. sustained role, Shulman et al., 2009) or because the same neuronal population may receive inputs from multiple afferents with different latencies (e.g., retinotectal vs. geniculostriate, Chambers et al., 2004; local vs. long-distance connections, Chambers & Mattingley, 2005). Recurrent cortico-cortical functional connections are known to characterize mechanisms of attentional selection (Kastner & Ungerleider, 2000; Duncan, Humphreys, & Ward, 1997; Desimone & Duncan, 1995) and mental imagery (Kosslyn, Ganis, & Thompson, 2001; Kosslyn et al., 1999).

Knowing the peak time of critical involvement across network areas may also unveil patterns of functional connectivity. Khayat, Pooresmaeili, and Roelfsema (2009), for example, recorded the temporal involvement of single FEF neurons during a covert attentional orienting task, followed by an overt oculomotor response. Two types of responses were detected in the covert attentional orienting phase: an early response reflecting visual processing and a later response that signaled the activity of a target selection mechanism. Interestingly, the visual response in FEF neurons seemed to occur later than in primary visual cortex (as recorded in a previous study, Khayat, Spekreijse, & Roelfsema, 2006), whereas the target selection response occurred at about the same time at the opposite ends of the visual cortical processing hierarchy. These findings suggest a profile of functional connectivity in which information passes from posterior to anterior in the earlier phase, followed by synchronized activity in the later phase. Analogous dynamics and attentional selection mechanisms may be involved in the generation of the SNARC effect.

To capture this potential interplay and biphasic temporal profile, we modeled our performance data with a biphasic Gaussian function that allows up to two periods of processing between −200 and 500 msec relative to stimulus onset (see also Stevens et al., 2009). Note that this is an adaptive modeling approach, as it enables the detection of two effect peaks in the stimulation time window but does not impose them (see also Chambers, Allen, Maizey, & Williams, in press).

Following Rusconi et al. (2011), disruption of the two frontal sites was expected to significantly reduce the SNARC effect in the context of number magnitude judgment whereas TMS of the PPC should mainly interact with explicit number magnitude processing and induce a neglect-like effect for smaller numbers (Göbel et al., 2006; Göbel, Walsh, & Rushworth, 2001; see also Oliveri et al., 2004). Furthermore, top–down processes may be involved in the mapping of number onto space, as shown, for example, by Galfano, Rusconi, and Umiltà (2006) in the case of spatial orienting effects induced by number magnitude processing, and as theorized by Fischer (2006) for the SNARC effect. In recalibrating mappings from numerical stimuli to lateralized spatial responses, which entail top–down control, it may be expected that the contribution of frontal areas to the SNARC effect would occur in the early phases of processing (e.g., Bardi, Kanai, Mapelli, & Walsh, 2012; O'Shea, Muggleton, Cowey, & Walsh, 2004).

On the basis of Corbetta and Shulman's (2011) model, timing and lateralization of effects was also expected to differentiate between the functional effects of the two frontal nodes, with the ventral node (rIFG) delivering the earlier signal when a (re)-Orienting Response (OR) was necessary (see also Corbetta & Shulman, 2002). In our experimental setting, this could be expected to happen on each trial, because participants were always fixating the center of the screen and with their mind's eyes on number 5 (reference number) at the beginning of each trial. Appearance of any different number, therefore, would trigger a "disengage and orient" response. Moreover, in accordance with Corbetta and Shulman's model, which postulates a role for FEF in contralateral orienting, and in light of Rusconi et al.'s (2011) findings from rTMS, the effects of rFEF TMS could be expected to become more evident with small than large numbers (see also Bardi et al., 2012, for evidence on a contralateral role of rFEF in spatial S-R correspondence). In contrast, rIFG TMS may be expected to affect both sides of the MNL (e.g., Rusconi et al., 2011).

METHODS

Participants

Twenty-one volunteers (10 women; mean age = 26 years, range = 20–37 years) participated in the study, of which 20 received TMS to rFEF, 18 to rIFG, and 18 to

rPPC. In total, 17 participants undertook the complete experiment, and four withdrew after receiving TMS to one or more sites. All participants were naive to the goals of the study, had normal or corrected-to-normal vision, and were right-handed. All experimental procedures met the ethical guidelines of the School of Psychology at Cardiff University and adhered to the Declaration of Helsinki.

TMS Parameters

TMS was administered with a Magstim Rapid2 system (Magstim Company, Whitland, UK) and a standard 70-mm figure-of-eight coil. The intensity of stimulation was initially set at 120% of the distance-adjusted individual resting motor threshold (see Stokes et al., 2005, 2007). If the initial target intensity exceeded individual discomfort thresholds, most likely when the coil was placed over rIFG, stimulation output was gradually reduced until it caused no discomfort and was then matched across all sites for a given subject. This procedure yielded an average stimulation of 113% of individual distance-adjusted individual resting motor threshold (range = 90–120%, SD = 11). Average stimulation intensity corresponded to 51% (SD = 7.6) of maximum stimulator output for rPPC, 49% (SD = 9.3) for rFEF, and 48% (SD = 8.1) for rIFG (see Appendix A for additional details and individual data on scalp–cortex distances). During the experiment, the coil was fixed in place by a mechanical coil holder (Manfrotto, Bassano del Grappu, Italy), and for all sites, the coil was positioned with the handle pointing in a posterior direction.

TMS Localization

Sites were localized in each participant's T1-weighted MRI scan, which was coregistered with the participant's scalp using a magnetic tracking device (miniBird 500; Ascension Tech; MR coregistration software: MRIReg). To stimulate rFEF, TMS was applied over the right posterior middle frontal gyrus, slightly anterior and ventral to the junction between superior frontal sulcus and the ascending limb of precentral sulcus in each individual, a location that corresponded with the anatomical delineation of rFEF (as in Muggleton, Juan, Cowey, & Walsh, 2003). The rIFG was stimulated in correspondence with BA 45/BA 47 in the area comprised between the pars triangularis and the inferior frontal sulcus (see Rusconi et al., 2011). Finally, the rPPC was localized in the area of the posterior intraparietal sulcus, as in Rusconi et al. (2007). These sites were initially localized by unnormalizing Montreal Neurological Institute (MNI) coordinates on individual brain scans through SPM5 (Wellcome Department of Imaging Neuroscience, University College London). This procedure involved normalizing each participant's T1-weighted MRI scan against a standard template. The description of each resulting transformation was then used to convert the appropriate MNI coordinates to the untransformed (native) anatomical coordinates, yielding subject-specific localization of the sites. Nearest cortical surface coordinates were then calculated for each site in each individual's native space and marked as target sites [nearest cortical surface targets across participants: rFEF (32, 3, 68) and rIFG (59, 24, 19), localized with Rusconi et al.'s (2011) reference coordinates, and rPPC (40, −76, 47), based on Rusconi et al.'s (2007) coordinates; see Figure 1, top and bottom]. Finally, such coordinates were then used to identify stimulation targets on scalp coordinates after scan-scalp coregistration.

Procedure

On each trial, participants fixated a central white cross on a black background. After 500 msec, the cross was replaced by a white central digit (range: 1–9, 5 excluded; font and size: Arial 48 Bold) subtending approximately 1.2° × 1.9° of visual angle and displayed for 1300 msec. Participants classified digits as smaller/larger than 5 by pressing a left key (corresponding to V on a qwerty keyboard) with the right index finger or a right key (corresponding to N) with the right middle finger. Participants were instructed to respond both rapidly and accurately. A 600-msec visual feedback screen ("Error" in case of incorrect or "Too Slow" in case of missing response) or blank screen (in case of correct response) followed and was then replaced by another 200-msec blank screen before the start of a new trial (see Figure 2).

Because the experimental set comprised numbers ranging from 1 to 9, numbers from 1 to 4 were considered small and numbers from 6 to 9 were considered large (Dehaene et al., 1993). In accordance with the SNARC effect, we thus expected to find a baseline advantage for left-key responses to 1–4 and for right-key responses to 6–9, as in Rusconi et al. (2011; see also Riello & Rusconi, 2011), where the same task and response arrangement were used. Trials were labeled as "compatible" when the correct response to small numbers was a left response and the correct response to large numbers was a right response. Vice versa, trials were labeled as "incompatible" when the correct response to small numbers was a right response and the correct response to large numbers was a left response.

The experiment was divided into four sessions per participant. The first session (~90 min) included training with the experimental task and measurement of individual resting motor threshold. The second, third, and fourth sessions were each devoted to stimulation of a different site and took on average 180 min each. Order of sites was counterbalanced between participants. Each session consisted of 14 TMS blocks. Half of the blocks were performed with a compatible S-R mapping, and half with an incompatible mapping. Compatible and incompatible blocks were presented in alternate order, and the starting

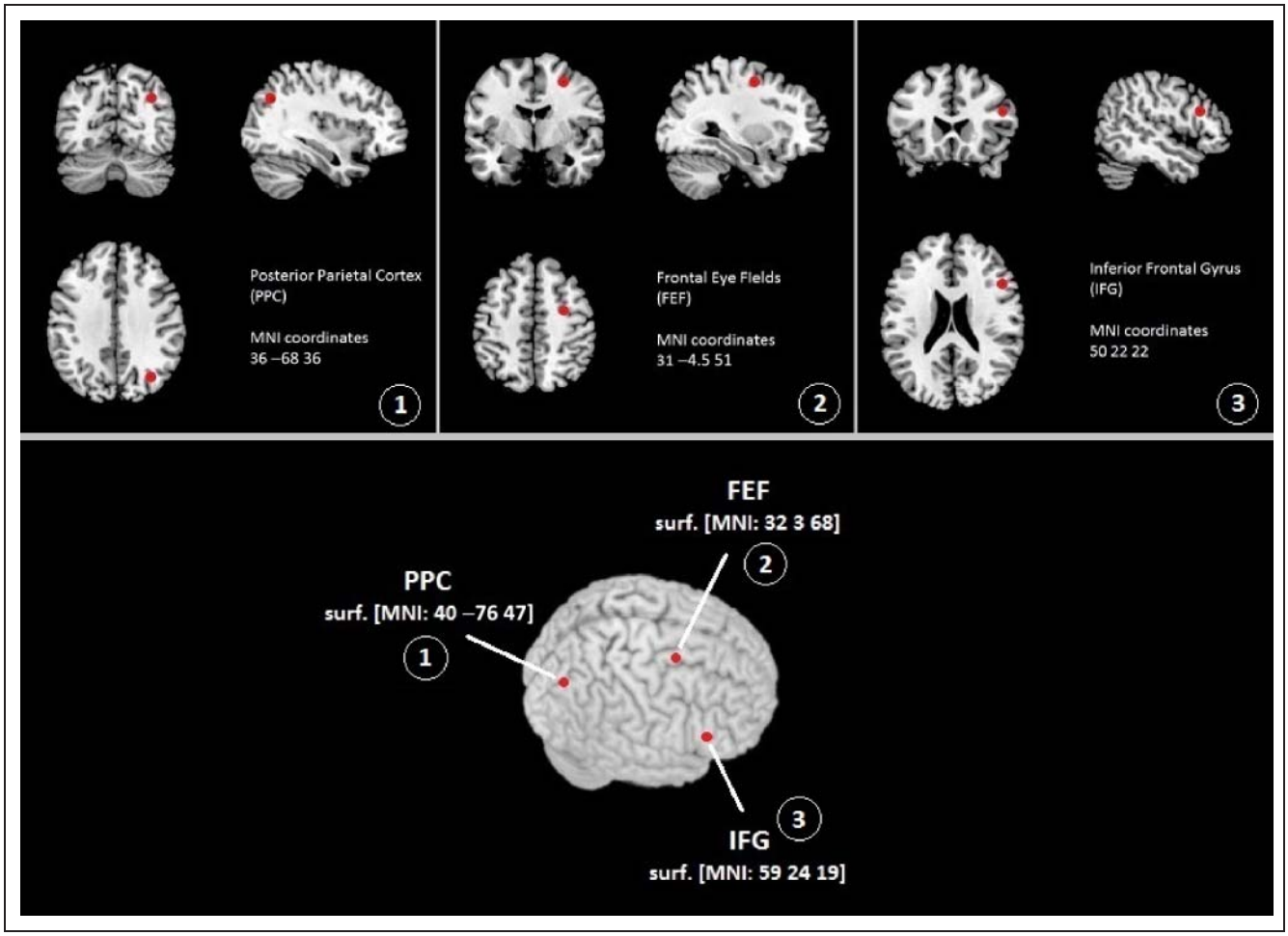

Figure 1. Target stimulation sites are shown in slice and 3-D templates along with their MNI coordinates. Original target points are shown on a template in the upper half of the figure; nearest cortical surface targets (identified by tracing a perpendicular segment between original targets and adjacent cortical surface) are shown in the bottom part of the figure. Stimulation was directed toward these latter points. To stimulate rFEF, TMS was applied over the right posterior middle frontal gyrus, slightly anterior and ventral to the junction between superior frontal sulcus and the ascending limb of precentral sulcus (see Muggleton et al., 2003). rIFG was stimulated in correspondence with BA 45/BA 47 in the area comprised between the pars triangularis and the inferior frontal sulcus (see Rusconi et al., 2011). The rPPC stimulation site was localized in the area of the posterior intraparietal sulcus as in Rusconi et al. (2007).

condition (i.e., either compatible or incompatible) was counterbalanced between participants. Each block consisted of 120 experimental trials including eight initial "buffer" trials (i.e., trials with no TMS to absorb behavioral costs associated with changes in S-R mapping, which were subsequently discarded). For each site, there were 1568 experimental trials in total (14 blocks × 112 experimental trials per block, including one trial per number magnitude [1,2,3,4,6,7,8,9] and TMS condition per block). TMS was delivered on 1456 of the trials at 1 of 13 different time points (0, 33, 67, 100, 133, 167, 200, 233, 267, 300, 333, 367, and 400 msec from stimulus onset; see Figure 2), whereas no TMS was delivered in the remaining 112 trials. Trials with TMS and without TMS were randomly intermingled throughout each block. Throughout each trial, gaze was monitored on-line with a Cambridge Research Systems 250 Hz eyetracker. Trials in which TMS caused a blink or gaze deviated more than 2° from fixation were discarded.

In addition, four to five blocks of sham stimulation (i.e., with the coil held perpendicular to stimulation site and the same TMS–noTMS conditions in a random fashion) were also included at the beginning of each session and then compiled across sessions into a single 14-block condition to separately assess the effects of the auditory click artifact on the number comparison task. In total, the design included 28 observations per cell of Site (Sham, FEF, IFG, PPC) × TMS (13 time points + no-TMS) × Compatibility (compatible, incompatible) × Number magnitude (<5, >5). The SNARC effect was operationalized as the difference between Incompatible and Compatible conditions (see Introduction; Mapelli, Rusconi, & Umiltà, 2003).

RESULTS

Response latency and accuracy were determined on a trial-by-trial basis. Across the entire data set, trials in which eye

movements or blinks (3.5% overall) occurred between stimulus presentation and response execution were excluded. Furthermore, to ensure that behavioral performance on TMS trials could potentially uncover the effects of brain stimulation, trials where the response was executed before TMS onset were excluded (4.95% overall; <2% for TMS SOAs up to 300 msec; 6.3% at 333 msec, 17.7% at 367 msec, and 36.5% at 400 msec). The latter two time points (367 and 400 msec) were subsequently excluded from all further analyses because of insufficient responses on TMS trials following TMS onset. To exclude the influence of any speed–accuracy trade-offs while summarizing performance in one single index, the dependent variable for behavioral analysis was adjusted median RTs (AdjRTs), calculated as median RT on correct trials divided by the proportion of correct responses in each cell of the design (Townsend & Ashby, 1983).

Measurement of Basic SNARC Effect

An initial analysis confirmed that the baseline SNARC effect (i.e., the difference between incompatible and compatible condition for no-TMS trials across sessions) was significant [$t(20) = 3.86$, $p < .001$; $M = 27$ msec, $SE = 7$; $r = .65$; Rosenthal, 1991]. For the 17 participants who took part in all sessions, a two-way repeated-measures ANOVA of baseline SNARC on no-TMS trials, including factors of Site (rPPC, rIFG, rFEF, sham) and Magnitude (small, large), did not detect any significant main effects or interactions (all Fs < 1.38, all ps > .25). This indicates that the SNARC effect in no-TMS trials was present and consistent across sites.

Nonlinear Regression on ΔSNARC

To determine the effect of cortical stimulation on the MNL, we computed the TMS-induced change in SNARC effect within sessions (ΔSNARC; i.e., the change in the difference between incompatible and compatible trials from no-TMS to TMS conditions). This measure was then entered in the following analyses. By design, the effects of TMS over rPPC, rFEF, and rIFG on the SNARC effect were investigated at 13 different SOAs with 33-msec increments (0–400 msec relative to the onset of a target number). As noted above, however, the two longest TMS time points (367 and 400 msec) were excluded from

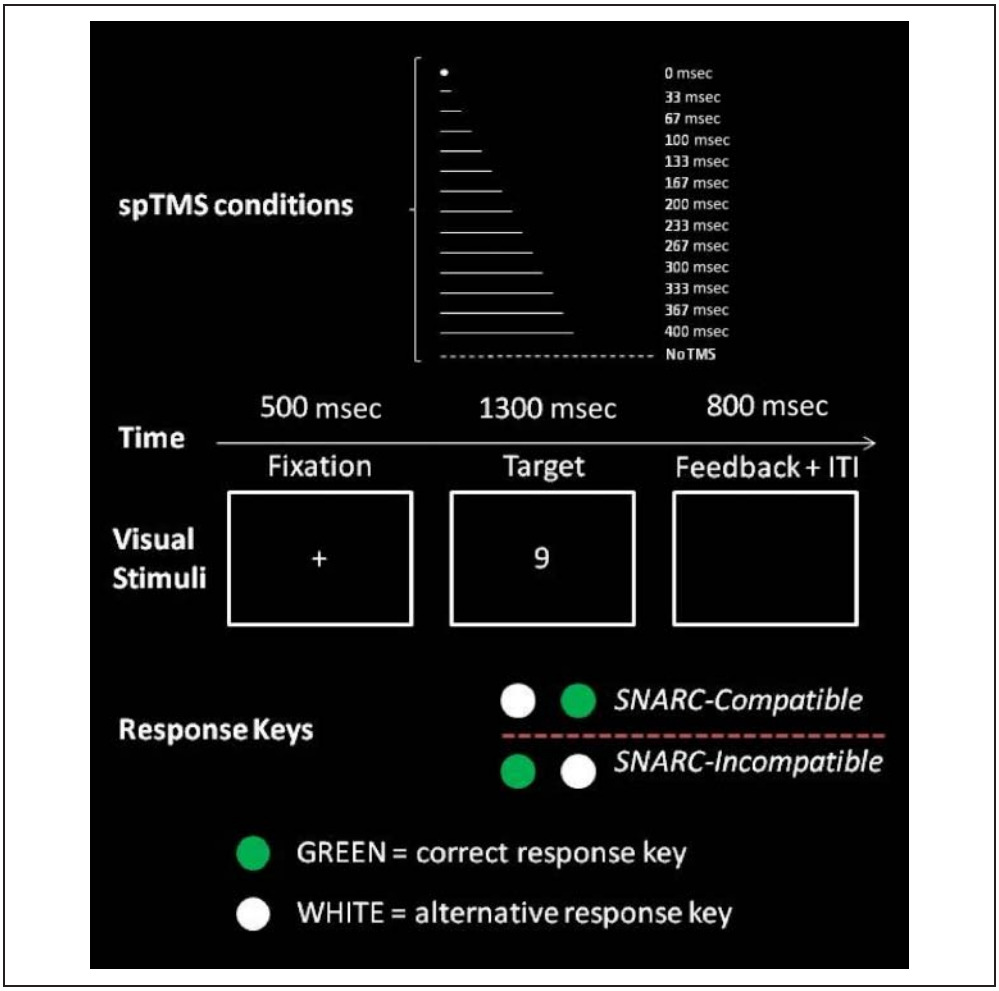

Figure 2. Trial structure is shown. On each trial participants fixated the center of a display where a digit (1–9, 5 excluded) appeared for 1300 msec. Digits were to be classified as smaller or larger than 5 by pressing one of two horizontal response buttons. Participants responded with their right index and middle fingers (i.e., with the hand ipsilateral to the stimulated hemisphere). Because the target 9 is large in the range of experimental stimuli, the right-side key is "compatible" on a left-to-right representation of numbers 1–9, and the left-side key is "incompatible." spTMS was delivered at 1 of 13 different timepoints and intermingled with no-TMS trials. spTMS = single-pulse TMS; ITI = intertrial interval.

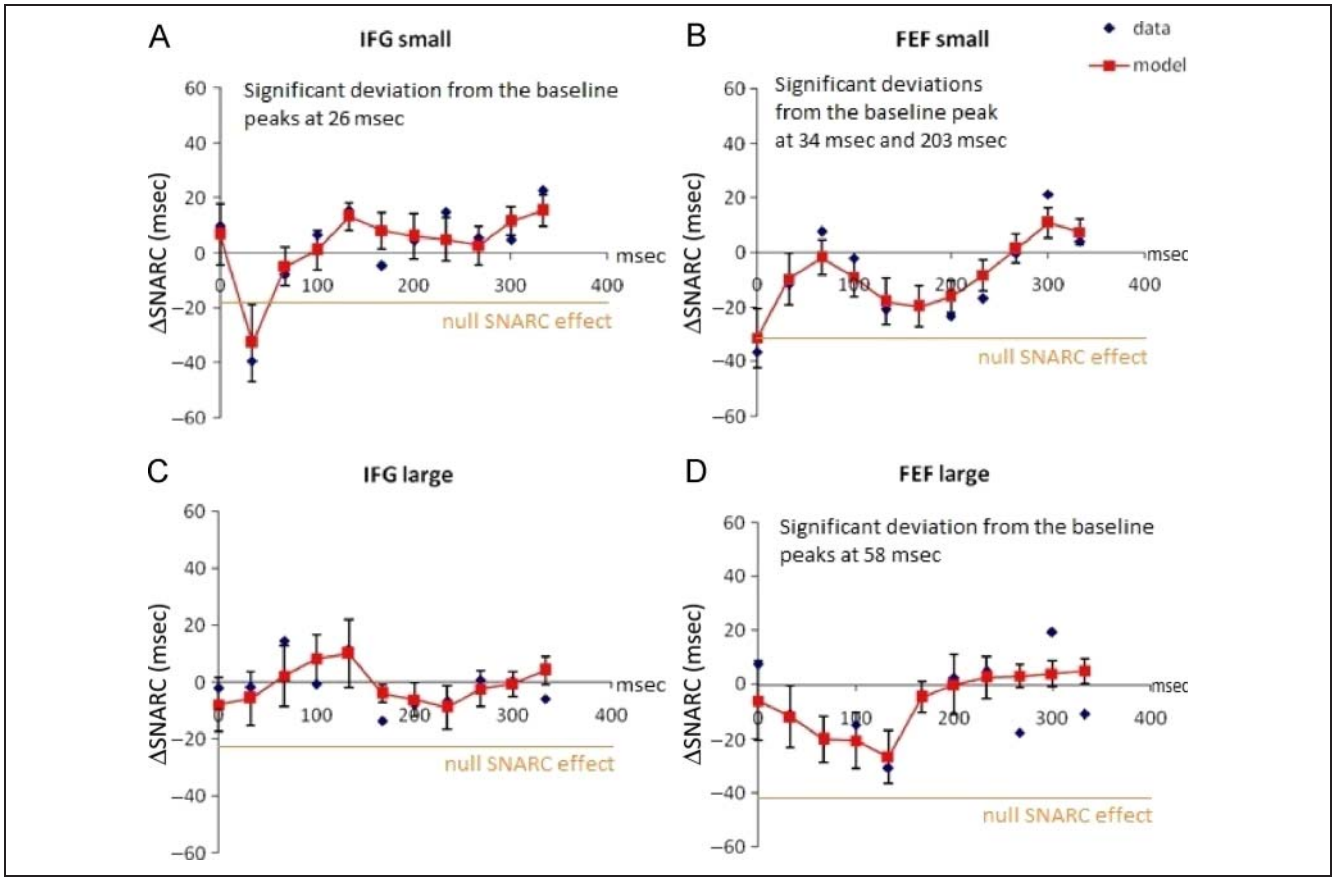

Figure 3. Group data in blue and curve fits in red (vertical lines indicate standard error of the model's mean) are shown for rIFG (A and C) and rFEF (B and D), that is, the sites where spTMS significantly reduced or suppressed the SNARC effect compared with the noTMS baseline (here corresponding to 0). Orange horizontal lines indicate the value of ΔSNARC, which would lead to a null SNARC effect. See Appendix C for plots of the sham and rPPC blocks and Table 1 for details about model parameters and goodness of fit.

the analyses on ΔSNARC because of insufficient trial numbers.

Individual data were fitted to a biphasic Gaussian model that permits up to two distinct epochs between −200 and +500 msec poststimulus onset to capture effects that may originate outside the 0–333 stimulation window (for a similar approach, see Stevens et al., 2009; Chambers et al., in press). Data were thus fit to the following model, composed of the sum of two Gaussian functions:

$$y = y_0 + a_1 e^{\left[-0.5\left(\frac{x-x_1}{b_1}\right)^2\right]} + a_2 e^{\left[-0.5\left(\frac{x-x_2}{b_2}\right)^2\right]}$$

where x is TMS onset in msec, x_1 and x_2 are the two peak TMS times that cause maximal deviation from ΔSNARC = 0, b_1 and b_2 are the Gaussian bandwidths (FWHM), a_1 and a_2 are the amplitudes (heights) of each Gaussian, and y_0 is the baseline performance level for which TMS disruption is minimal (see Appendix B for a specification of the constraints imposed to curve fitting on individual data). Group data and curve fits, derived from the means of the fitted parameters values, are shown in Figure 3 for relevant sites in the ΔSNARC analysis, whereas all parameter specifications can be found in Table 1. Note that the baseline-corrected amplitude (a_1 and a_2) was calculated by subtracting the baseline change in SNARC (y_0) from the corresponding amplitude parameter, for a particular combination of TMS site and Gaussian phase (first or second). This measure is optimally suited to establish the time course of critical effects, because it eliminates any time nonspecific influences of TMS that might elevate or reduce the SNARC effect.

The models accounted for 59–73% of the variance in each subcondition of TMS site (rFEF, rIFG, rPPC, sham) and number magnitude (small, large; see Table 1). For rIFG, this analysis revealed a significant TMS-induced reduction of the SNARC effect for small numbers in the first phase of the fitted function, peaking rapidly at +26 msec (mean $a_1 = -43.7$ msec, $p < .02$; Figure 3A and Table 1). No significant modulation of rIFG TMS was observed on the SNARC effect for large numbers (see Figure 3C and Table 1). Note that this modeling approach fits a continuous function to a discrete sampling protocol; therefore, peak times do not necessarily overlap with stimulation time points.

For rFEF stimulation, corresponding reduction in the SNARC effect for small numbers was found in both phases, with peaks at +34 and +203 msec (mean $a_1 = -40.5$ msec, $p < .02$; mean $a_2 = -44$ msec, $p < .01$; Figure 3B and Table 1). Modulation of the SNARC effect was also found for large numbers in the first phase for rFEF stimulation, peaking at +58 msec (mean $a_1 = -59.2$ msec, $p < .005$; Figure 3D and Table 1). No significant effects were found either in the Sham control condition or when TMS was delivered on rPPC (see Table 1 and Appendix C).

Nonlinear Regressions on ΔAdjRT for Compatible and Incompatible Trials

The reported ΔSNARC effects could derive from (a) enhanced performance in the incompatible condition and/or (b) disrupted performance in the compatible condition. Further modeling of ΔAdjRT (i.e., the difference between TMS and no-TMS trials irrespective of SNARC correspondence) was therefore undertaken for the sites and conditions where a significant modulation of the SNARC effect was found.

The models accounted for 57–72% of the variance in each subcondition of TMS site (rFEF, rIFG), number magnitude (small, large), and compatibility (compatible, incompatible; see Table 2). For rIFG, the reduction in SNARC for small numbers in the early phase was because of impairment on compatible trials peaking at 46 msec (mean $a_1 = +45.2$ msec, $p < .005$; Table 2). For rFEF, the analyses revealed that, for small numbers in the early phase, the SNARC reduction stemmed from both facilitation on incompatible trials and impairment on compatible trials (incompatible condition: peak time = 75 msec; mean $a_1 = -31.3$ msec, $p < .02$; compatible condition: peak time = 88 msec; mean $a_1 = +29.9$ msec, $p < .05$; see Table 2). However, for the later phase of rFEF, the reduction in SNARC for small numbers was driven wholly by facilitation on incompatible trials (peak time = 225 msec; mean $a_2 = -36$ msec, $p < .01$; see Table 2). For large numbers, the SNARC reduction in the early phase was because of impairment on compatible trials (peak time = 72 msec; mean $a_1 = 40.6$ msec, $p < .005$; Table 2).

Finally, note that all of the effects detected with nonlinear regressions for compatible and incompatible trials separately confirmed our previous analyses on ΔSNARC (i.e., analyses on a combined index); however, they appeared to peak at a later time than the effects detected on ΔSNARC (see Tables 1 and 2). Such forward shifts may be either because of random variation, in which case no significant difference is expected between peak times in the analysis on ΔSNARC versus peak times in the analysis on ΔAdjRTs or alternatively to systematic effects of a combined contribution from the compatible and incompatible conditions that significantly anticipates peaks in the analysis on ΔSNARC. We thus performed paired t tests to discriminate between these two hypotheses. No significant differences were observed between peak times for the ΔSNARC and ΔAdjRTs effects in the rIFG small number condition, rFEF large numbers condition, and rFEF small numbers condition for the late phase (all ps > .24). Peak times in the first phase of the rFEF small number condition (compatible: $M = 88$ msec, $SEM = 14$; incompatible: $M = 75$ msec, $SEM = 14$) were significantly different from those of the rFEF small number condition in the

Table 1. Mean (*SEM*) Parameters (in msec) Extracted from Double-Gaussian Regression Analyses of SNARC

				First Period			*Second Period*		
Site	*Magnitude*	R^2_{MEAN}	R^2_{TOTAL}	a_1	x_1	b_1	a_2	x_2	b_2
rFEF	Small	0.71 (0.02)	0.94	**−40.5 (15)***	33.8 (9.7)	25.8 (4.4)	**−44 (14.3)****	202.9 (13.1)	26.5 (5.4)
	Large	0.66 (0.04)	0.67	**−59.2 (17.1)*****	57.7 (11.3)	24.5 (7)	−20.1 (16.3)	N/A	N/A
rIFG	Small	0.73 (0.03)	0.92	**−43.7 (16.2)***	26.3 (8.9)	23.8 (5.1)	−16.8 (13.6)	N/A	N/A
	Large	0.69 (0.03)	0.56	−18.6 (17)	N/A	N/A	−2.4 (17.3)	N/A	N/A
rPPC	Small	0.61 (0.02)	0.56	−3.2 (17)	N/A	N/A	−4.3 (14.3)	N/A	N/A
	Large	0.59 (0.04)	0.78	6.5 (15.9)	N/A	N/A	−10.6 (17.1)	N/A	N/A
Sham	Small	0.65 (0.04)	0.53	−0.7 (16)	N/A	N/A	−15.9 (15.2)	N/A	N/A
	Large	0.64 (0.04)	0.77	−10.6 (16.1)	N/A	N/A	−3.1 (14.2)	N/A	N/A

Mean and total goodness of fit values are also provided for data modeling (R^2_{MEAN} and R^2_{TOTAL}, respectively). Significant key parameters (difference from zero) are indicated by asterisks. Note that peak times and bandwidths are interpretable only when the peak amplitude is also significant.

a = baseline-corrected amplitude; x = peak time; b = bandwidth.

*$p < .02$.

**$p < .01$.

***$p < .005$.

Table 2. Mean (*SEM*) Parameters Extracted from Double-Gaussian Regression Analyses of AdjRT (Separated According to Response Compatibility)

					First Period			*Second Period*		
Site	*Magnitude*	*Compatibility*	R^2_{MEAN}	R^2_{TOTAL}	a_1	x_1	b_1	a_2	x_2	b_2
rFEF	Small	Comp	0.68 (0.03)	0.80	**29.9* (12.6)**	88.2 (14.2)	16.0 (3.0)	−12.7 (11.3)	N/A	N/A
		Incomp	0.57 (0.03)	0.80	**−31.3* (11.6)**	75.0 (13.7)	29.6 (7.1)	**−36.0****	225.2 (12.7)	26.7 (4.7)
	Large	Comp	0.72 (0.03)	0.91	**40.6*** (12.0)**	71.7 (13.1)	21.0 (5.5)	10.2 (16.0)	N/A	N/A
		Incomp	0.65 (0.04)	0.89	2.8 (17.6)	N/A	N/A	4.9 (13.4)	N/A	N/A
rIFG	Small	Comp	0.64 (0.05)	0.98	**45.2*** (13.2)**	46.2 (8.6)	24.1 (5.1)			
		Incomp	0.61 (0.05)	0.73	24.2 (15.4)	N/A	N/A			
	Large	Comp	0.68 (0.03)	0.80	**45.7*** (11.3)**	56.2 (9.2)	21.9 (7.0)			
		Incomp	0.67 (0.04)	0.94	**62.2*** (12.8)**	27.5 (8.4)	38.9 (12.5)			

Mean and total goodness of fit values are also provided for data modeling (R^2_{MEAN} and R^2_{TOTAL} respectively). Significant key parameters (difference from zero) are indicated by asterisks. Note that peak times and bandwidths are interpretable only when the peak amplitude is also significant.

a = baseline-corrected amplitude; x = peak time; b = bandwidth.

*$p < .02$.

**$p < .01$.

***$p < .005$.

ΔSNARC analysis (M = 34 msec, SEM = 10; $t(19)$ = 3.35, p = .003 and $t(19)$ = 3.73, p = .001, respectively). Thus, the significant effect on small numbers in the first period of rFEF stimulation peaked earlier when compatible and incompatible trials were collapsed in the ΔSNARC analysis. This was most likely because of the combination of separate subthreshold effects on both compatible and incompatible trials. The apparent delay in the peak times of the remaining effects in the ΔAdjRTs analysis, instead, can be treated as random variation.

Linear Regression Analyses to Test for Potential rIFG-rFEF Functional Connectivity

From previous analyses, it emerged that TMS on rIFG disrupted SNARC in an early phase only, whereas TMS over rFEF disrupted SNARC both in an early and in a late phase. Here we explored the possibility that the early rIFG-TMS and the later rFEF-TMS effects might tap on connected functional circuits. If that was the case, later rFEF-TMS effects may be partly predicted by earlier rIFG-TMS effects.

Exploratory analyses revealed that the early rIFG and the latest rFEF effect may indeed be related and their relation may be specific (i.e., no other significant relations were found between rIFG-TMS and rFEF-TMS effects; see Appendix D). We therefore assessed that relation directly between the actual sources of the rIFG and rFEF effects: the SNARC-compatible condition for the early rIFG-TMS effect and the incompatible condition for the later rFEF-TMS effect. This fine-grained analysis confirmed that the amplitude of the rIFG effect predicted the amplitude of the later rFEF effect for small numbers (R^2 = .34, p = .01; see also Figure 4B) and that the peak time of the rIFG effect predicted the peak time of the later rFEF effect for small numbers (R^2 = .25, p = .04; see also Figure 4C). The regression on peak times shows that a positive linear relation exists between the peak time of the early effect on rIFG and the peak time of the later effect on rFEF (see Figure 4C). As for the direction of the relation between amplitudes, Figure 4B shows that a large slowing of the SNARC-compatible condition with rIFG-TMS in the early phase predicts a large facilitation of the SNARC-incompatible condition with rFEF-TMS in the late phase.

Nonlinear Regression Analyses on ΔAdjRT Collapsed across Compatibility Conditions

To assess the presence of TMS effects specific to number magnitude, data were collapsed across SNARC compatibility and the same modeling approach as for the SNARC analysis was applied to detect TMS-induced changes in overall adjusted median RTs relative to the site-specific noTMS condition (ΔAdjRT). Because of collapsing compatible and incompatible trials, sufficient TMS data were now obtained at later TMS SOAs to permit the inclusion of the +367 msec condition. We will report here below and in Table 3 only the results for those sites where a change in AdjRT occurs without any concomitant effects on SNARC, which would render uninterpretable any results collapsed across compatibility. The complete version of this analysis can be found in Appendix E.

The model accounted for 60–70% of the variance in each subcondition of TMS site and number magnitude

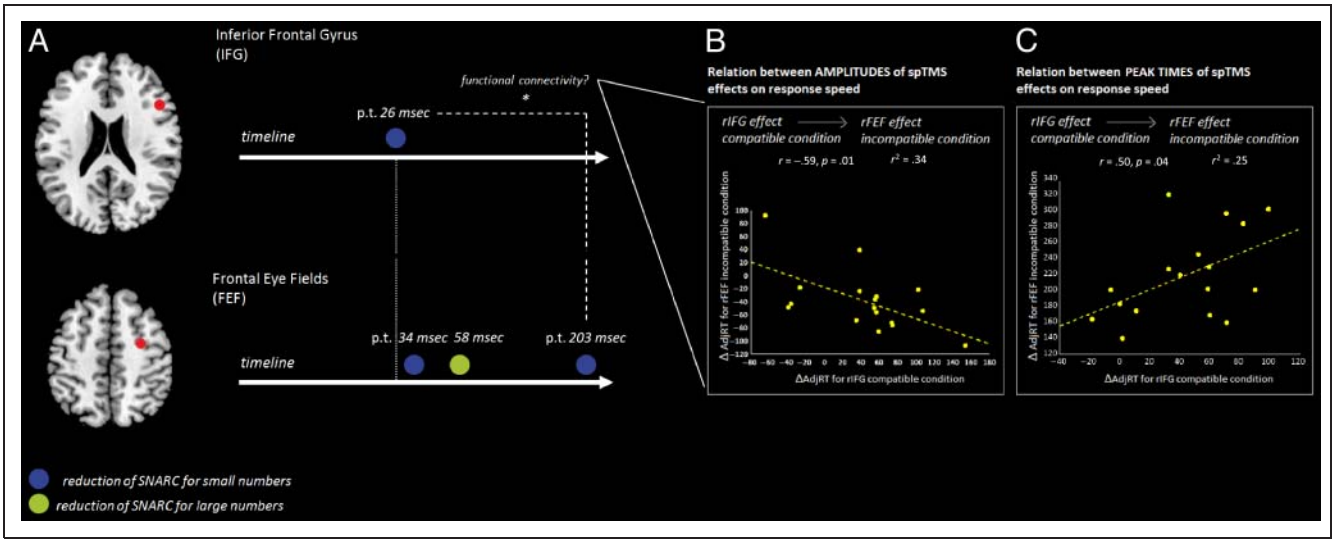

Figure 4. (A) A graphical representation is provided, summarizing the effects of TMS over the anterior sites on ΔSNARC. Linear regression established a significant relation between the early rIFG effect and the late rFEF effect. (B) Finer-grained analyses on the sources of the effects on ΔSNARC for rIFG and rFEF revealed that the amplitude of the early rIFG effect for small numbers (compatible condition) can explain up to 34% of the late rFEF effect for small numbers (incompatible condition), as shown in the scatterplot. (C) Finer-grained analyses on the sources of the effects on ΔSNARC for rIFG and rFEF revealed that the peak time of the early rIFG effect for small numbers (compatible condition) can explain up to 25% of the latency of the rFEF effect for small numbers (incompatible condition), as shown in the scatterplot.

(small, large; see Table 3). No significant TMS effects were found in the sham condition (see Figure 5 and Table 3). Stimulation of rIFG generally impaired performance. For small numbers, the significant early slowing (peak time$_1$ = +49 msec; mean a_1 = 37 msec, $p < .005$; see Figure 5C) corresponds to the modulation of the SNARC effect, which was reduced because of a differential slowing on compatible trials and will not be further taken into account. For large numbers, rIFG stimulation also slowed performance both when applied early and also when applied at a later stage (peak time$_1$ = +28 msec; mean a_1 = 42 msec, $p < .01$ and peak time$_2$ = +219 msec; mean a_2 = 30 msec, $p < .005$; see Table 3 and Figure 5D). In this case, there was no concomitant modulation of SNARC and the TMS-induced impairments are therefore not ambiguous, as for small numbers.

Clear and opposing effects of rPPC stimulation were observed for small versus large numbers. For small numbers, significant interference from TMS was found in the initial phase, peaking at +61 msec (a_1 = 44.8 msec, $p < .005$; Figure 5A). For large numbers, on the contrary, significant TMS-induced facilitation was observed in the second phase, peaking at +197 msec (mean baseline-corrected $a_2 = -26.2$ msec, $p < .005$; Figure 5B).

Linear Regression Analyses to Test for Potential rIFG-rPPC Functional Connectivity

Nonlinear Regression Analyses on ΔAdjRT Collapsed across Compatibility Conditions section revealed interpretable effects of TMS on overall performance for rPPC (early impairment of small number processing and late facilitation of large number processing) and rIFG (early and late impairment of large number processing).

Simple linear regressions were thus performed with either the amplitude of the earliest significant effect or its peak time (rIFG large; ΔAdjRT = 41.7; *SEM* = 10; peak time: *M* = 28.3 msec; *SEM* = 10.6; see Table 3) as predictors and the amplitudes and peak times of the later effects of rPPC stimulation as dependent variables. Such analyses revealed that the amplitude of the early rIFG interference effect for large numbers predicted the amplitude of the later rPPC facilitation effect for large numbers (R^2 = .49, p = .002; see Figure 6). No other effects approached significance (all ps > .14).

DISCUSSION

The aim of this study was to reassess and extend recent evidence of the causal involvement of right frontal cortex (both dorsal and ventral nodes) in the mapping of number magnitude on lateralized responses by using a TMS protocol with optimized temporal resolution. We also aimed to differentiate the contribution of right frontal cortex from the contribution of rPPC, which is also thought to have a privileged connection with mental number space.

Rusconi et al. (2011) reported effects of rTMS on frontal sites in a magnitude comparison task but not in a parity judgment task; therefore, our in-depth analysis here focused on magnitude comparison. To best capture the typical activity pattern of nodes in frontoparietal networks, data were fitted to a biphasic inverse Gaussian function (as in Chambers et al., in press; Stevens et al., 2009; see also Introduction and Chambers & Mattingley, 2005). This approach has the key advantage of distilling the complex chronometry of TMS effects into a concise series of parameters, while also producing a faithful representation of the time-course of TMS effects. Our analysis produced parameters from two phases for each site: an earlier and a later phase. As predicted on the basis of previous evidence, anterior sites (rIFG and rFEF) were found to play a key role in the SNARC effect. The rPPC, however, interacted with number magnitude processing and in a "lateralized" manner (i.e., the effect was selective for either

Table 3. Mean (*SEM*) Parameters Extracted from Double-Gaussian Regression Analyses of AdjRT (Collapsed across Response Compatibility)

				First Period			*Second Period*		
Site	*Magnitude*	R^2_{MEAN}	R^2_{TOTAL}	a_1	x_1	b_1	a_2	x_2	b_2
rIFG	Large	0.64	0.85	**41.7*** (10)**	28.3 (10.6)	45.6 (14.6)	**29.8*** (8.9)**	218.6 (12.8)	22.3 (4.2)
rPPC	Small	0.70	0.9	**44.8 (9.7)*****	61.5 (12.7)	25.1 (5.8)	−2.6 (8.4)	N/A	N/A
	Large	0.60	0.87	0.5 (11.2)	N/A	N/A	**−26.2 (6)*****	196.8 (15.2)	74.6 (15.2)
Sham	Small	0.65	0.84	9.9 (10.4)	N/A	N/A	3.4 (9.4)	N/A	N/A
	Large	0.63	0.77	6.2 (10.2)	N/A	N/A	11.6 (9.8)	N/A	N/A

Mean and total goodness of fit values are also provided for data modeling (R^2_{MEAN} and R^2_{TOTAL}, respectively). Significant key parameters (difference from zero) are indicated by asterisks. Note that peak times and bandwidths are interpretable only when the peak amplitude is also significant. Only site where the effect is not confounded by concomitant effects on SNARC are reported. See Appendix E for an integral version of this table.

a = baseline-corrected amplitude; x = peak time; b = bandwidth.

***$p < .005$.

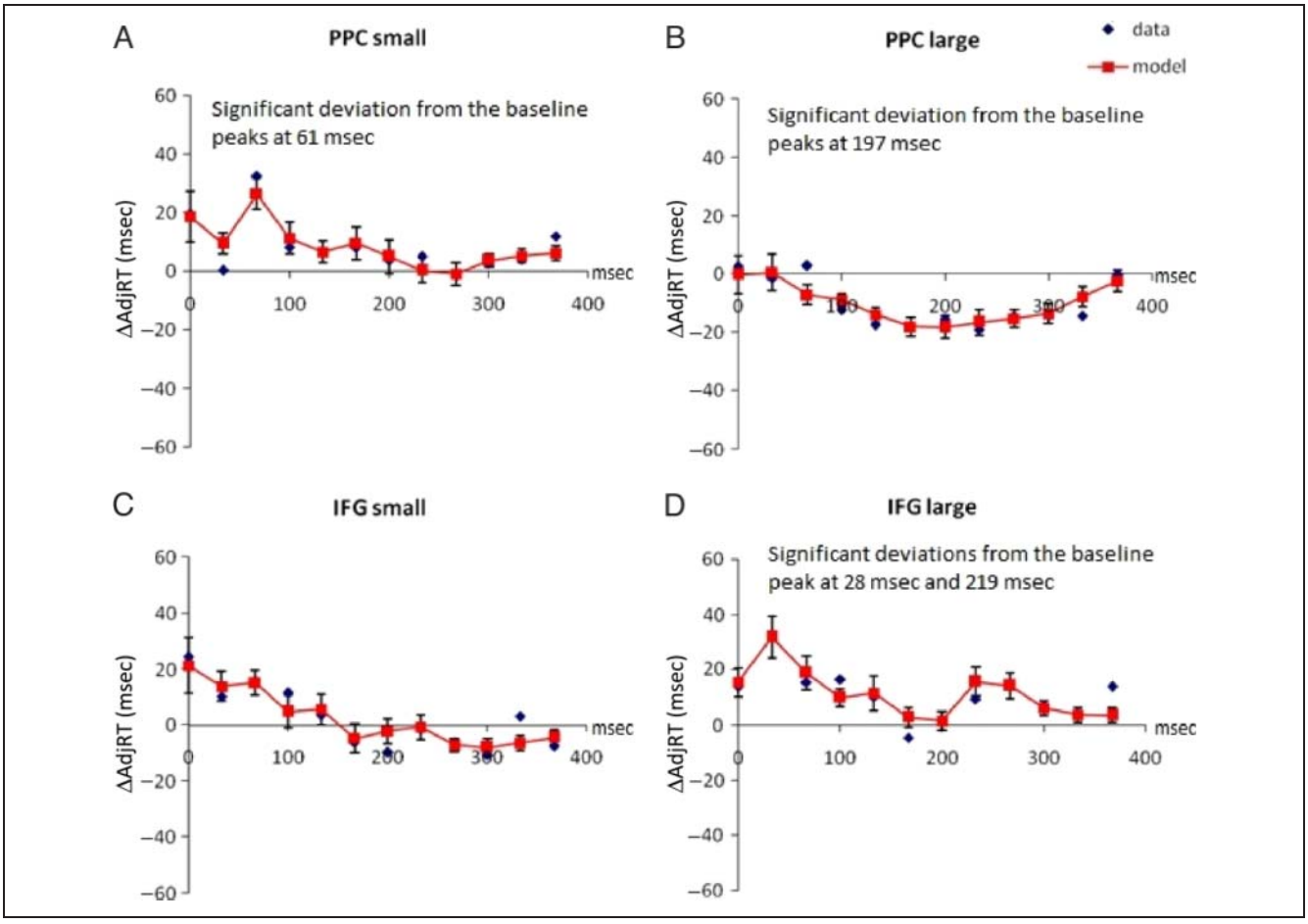

Figure 5. Group data in blue and curve fits in red (vertical lines indicate standard error of the model's mean) are shown for rPPC (A and B) and sham (C and D). Model parameters and goodness of fit are reported in Table 3.

small or large numbers) irrespective of response location. It thus seems that rPPC is crucial for either the mental representation of numbers in space or the deployment of spatial attention along such representations, whereas rFEF and rIFG permit the crosstalk between spatial codes assigned to numbers and lateralized response codes.

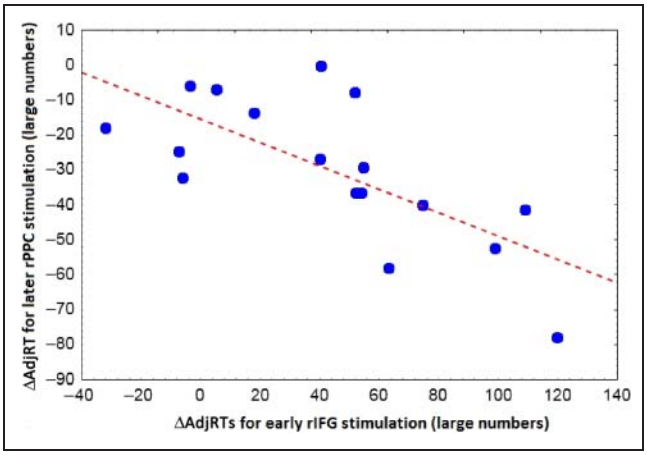

Figure 6. Scatterplot showing a significant relation between the amplitude of early rIFG effect for large numbers (interference) and the amplitude of the late rPPC effect for large numbers (facilitation).

Stimulation of rFEF suppressed the SNARC effect more effectively for small numbers than large numbers, which is consistent with Rusconi et al. (2011; also see Bardi et al., 2012, for spatial S-R correspondence). In the current study, however, we also found a significant effect of rFEF stimulation on the SNARC effect for large numbers, although it was restricted to the earlier phase. This is not at odds with the available literature, as rFEF stimulation has previously been shown to have bilateral effects on attentional orienting in physical space (e.g., Muggleton et al., 2003; Grosbras & Paus, 2002).

Moreover, we also confirmed a role for rIFG in the SNARC effect when number magnitude (and its supposedly connected mental spatial representation) is task relevant. This appears fully consistent with the documented involvement of the monkey ventral pFC (Rao, Rainer, & Miller, 1997) and human IFG (Rizzuto, Mamelak, Sutherling, Fineman, & Andersen, 2005) in spatially selective motor acts with task-relevant goals. It may be that scalp–cortex distance correction and the use of a single pulse rather than rTMS protocol made the effect of stimulation more selective than

in Rusconi et al. (2011), who found that rIFG suppressed the SNARC effect in both small and large numbers.

It has been proposed that rIFG and rFEF are important nodes of two reciprocally interconnected circuits governing attentional selection and spatial orienting. In particular, the ventral and right-lateralized circuit to which rIFG belongs has been suggested to act as a "circuit breaker" for triggering selection of targets in unattended locations (e.g., Corbetta & Shulman, 2002, 2011). The detection and OR toward task-relevant stimuli and characteristics (e.g., number magnitude and its location on the MNL) may therefore be one of its functions (or the direct consequence of its functions). Its role as a circuit breaker implies the possibility to bias activity in connected dorsal nodes. It therefore follows that earlier activity in the ventral circuit may contribute to later activity in the dorsal circuit. To assess in a simple way whether our TMS effects could be consistent with this functional connectivity model, we tested whether the parameters (amplitude and peak time) of the early effect on rIFG could predict the parameters (amplitude and peak time) of later effects on rFEF.

A first analysis on ΔSNARC was instrumental for detecting a possible connection and a subsequent analysis of ΔAdjRT—restricted to the sources of TMS effects on ΔSNARC (see Linear Regression Analyses to Test for Potential rIFG-rFEF Functional Connectivity section)—helped to disambiguate the direction and significance of this coupling. These analyses revealed that the early (peak time = +26 msec) reduction of the SNARC effect for small numbers during rIFG stimulation was significantly related to the late (peak time = +203 msec) reduction of the SNARC effect for small numbers during rFEF stimulation, whereas it was unrelated to rFEF-TMS effects at an earlier stage. Sources of this relationship within the SNARC effect were a significant slowing of AdjRTs in the compatible condition for small numbers with rIFG early stimulation and a significant facilitation of AdjRTs in the incompatible condition for small numbers with rFEF late stimulation. The relation between the defining parameters for these more specific effects was therefore assessed and the amplitude of the rIFG effect was found to explain 34% of the variance in the amplitude of the rFEF effect and 25% of the variance of the rFEF peak time. Specifically, greater impairments on compatible trials during early rIFG stimulation were associated with greater speeding on incompatible trials during late rFEF stimulation, and the peak time of the rIFG effect correlated positively with the peak time of rFEF effect (see Figure 4B and C). This suggests that, in normal conditions (i.e., in the noTMS baseline), stronger facilitation of small numbers on a left response is associated with stronger inhibition of small numbers on a right response. In other words, the extent of the compatible condition advantage is directly related to the extent of the incompatible condition disadvantage for the same stimulus.

One possible explanation for this relationship is the concerted working of two different mechanisms. The enhancement of a task-relevant compatible coupling between stimulus and response characteristics (facilitation mechanism) would crucially rely on rIFG activity, whereas the inhibition of the correct but incompatible response by the alternate response (reciprocal inhibition mechanism) would crucially rely on rFEF activity. From a more general perspective, this requires a functional connection projecting from rIFG to rFEF. According to Corbetta et al. (2008), it is precisely at the level of the right inferior/middle frontal gyrus that the ventral and the dorsal attention networks come to interact. When task-relevant input is detected, the ventral network locks in and acts as a circuit breaker by automatically selecting the new target with its associated spatial response (which may produce net facilitation) and modulating activity in the dorsal network. In turn, the dorsal network would then initiate an intentional OR toward the target. When the side of the OR does not match with the side of the correct response, a conflict would be generated (which may produce net interference) and need to be solved before response execution. Such a functional connectivity model, with distinct stages of compatible response activation and competitive response inhibition, is also consistent with an early and prototypical computational model of S-R spatial correspondence effects (see Zorzi & Umiltà, 1995). That model originally distinguished between a feed-forward automatic response activation stage and a later response selection stage. The activation strength of a spatially corresponding response determines the extent of inhibition received by a spatially noncorresponding response later on. We suggest that the mechanisms proposed in that early model for a spatial correspondence effect may be biologically plausible and applicable to the SNARC effect in a magnitude comparison task.

In contrast to the effects of frontal stimulation, the results during rPPC TMS exhibit a pattern that is reminiscent of the hemispatial neglect syndrome. Unilateral spatial neglect is characterized by an asymmetrical deficit in space processing (along with other nonspatial deficits; Husain & Rorden, 2003) in which neurological patients ignore stimuli presented in their left visual field, while processing the same stimuli when presented to their right visual field. This imbalance in the processing of stimuli in physical space often extends to the processing of stimuli in representational space (e.g., Bisiach & Luzzatti, 1978), and in some patients it extends to the number continuum (see e.g., Zorzi et al., 2002). It is therefore reasonable to assume that our participants were impaired in responding to small numbers (whatever the side of the response key), because their spatial attention/representation was biased away from the left visual field, where smaller numbers are expected to be mapped on the MNL. On the other hand, the facilitation found in responding to large numbers would mirror the common finding of biased processing of stimuli in the right visual field (often referred to as right hyperattention, e.g., Heinen et al., 2011; Hilgetag, Théoret, & Pascual-Leone, 2001), which is where larger numbers should be mapped on to the MNL. Our overall

pattern of results is consistent with previous studies that simulated a neglect-like bias in number space by applying rTMS on rPPC with different protocols (e.g., Göbel et al., 2006; Oliveri et al., 2004).

The opposing effects we find of rPPC-TMS in the early versus late phase of a trial (i.e., early interference with small number processing, late facilitation for large number processing) could be accommodated by current models of unilateral spatial neglect. Corbetta and Shulman (2011), for example, ascribe contralateral deficits to hypoactivation in the right dorsal network after lesions to functionally connected right ventral areas, which would subserve a bilateral role. The net deficit, however, would stem from interhemispheric interaction rather than single-hemisphere bias (e.g., Sylvester, Shulman, Jack, & Corbetta, 2007; see also Brighina et al., 2003). Under normal conditions, an initial OR toward a task-relevant target in the left visual field will be maintained until the target has been fully processed by applying a certain amount of inhibition to a spontaneous re-OR in the opposite direction. If however the initial OR (in our case toward the standard ["5"]) is weak, then the inhibition applied to the opposite hemisphere mechanism may also be weak. This could produce a rebound orienting and hyperattention toward the opposite hemifield. We can speculate, therefore, that a functional imbalance introduced by brain damage or TMS could produce both an early processing deficit for stimuli in the contralesional side and a later processing advantage for stimuli in the ipsilesional side. Alternatively, it is possible that rPPC is primarily critical for contralateral number representation (hence the early deficit) but that it also has an interhemispheric role (e.g., Heinen et al., 2011). Such a role would take longer to emerge, hence the late facilitation effect possibily because of disinhibition of the left hemisphere.

Regression analyses for TMS-induced effects on rIFG and rPPC, moreover, are consistent with these nodes being part of an interconnected ventral frontoparietal attention network. There appears to be a direct relation between the early engagement of rIFG for large numbers (as indicated by the amplitude of TMS disruption in the early phase) and the later facilitation for large number processing caused by TMS over rPPC. Unlike with rPPC effects, it would be difficult to speculate on the reasons why rIFG appears to be only involved in the processing of ipsilateral space (i.e., large numbers), independent from S-R compatibility, as well as in the compatibility effect for contralateral space only (i.e., small numbers). Rusconi et al. (2011), for example, had found an involvement of the rIFG for both the SNARC effect for small numbers and the SNARC effect for large numbers. No significant effect on collapsed RTs was found with rIFG-rTMS. Moreover, in that study, TMS intensity was not adjusted for site-specific differences in scalp–cortex distance. It is possible, therefore, that slightly different neuronal populations were targeted with these different TMS protocols and that they were reached with different stimulation strengths. Our rIFG site lies very close to the area that may contain mixed neuronal populations that are respectively connected with dorsal and ventral regions (Fox, Corbetta, Snyder, Vincent, & Raichle, 2006) and may be the main cortical interface—if not the only one—between ventral and frontal attentional networks (Corbetta et al., 2008). This may be the reason why rIFG is found to subserve a hybrid role and contributes both to S-R compatibility effects and to response-independent representations of mental number space when task-relevant. Consistently with this proposed hybrid role, rIFG early activity influenced both posterior ventral (rPPC) and anterior dorsal (rFEF) later activity.

Taken together, our findings confirm a rapid, critical and interconnected role of the rFEF and rIFG in the mapping of numbers on to response selection, and a critical role of both the rPPC and rIFG in either maintaining or exploring a mental representation of number space. What precise mechanisms and functional relations may underlie this frontoparietal processing network is still an open question, which may be best addressed in future studies by adopting a combined TMS-neuroimaging approach or multiple-coil stimulation protocols. These paradigms would enable concurrent tracking the flow of function and information processing through all of the identified critical nodes. Another outstanding question concerns the possible hemispheric specialisation for the mental representation of numbers in magnitude versus parity judgment tasks. On the basis of Gevers et al.'s (2010) proposal of a left-hemispheric origin for the SNARC effect in parity judgments, a right hemispheric origin for the SNARC effect in magnitude judgment, and on reported dissociations between the SNARC effects in parity and magnitude judgment during rTMS on the right frontal lobe (Rusconi et al., 2011), one may expect a specific left hemispheric involvement in the SNARC effect with parity judgments.

APPENDIX A

Individual Data Are Shown for Motor Threshold (MT), Scalp–Cortex Distance in Each Site, and Availability of Data Per Each Site

Subject	*Sex*	*Age*	*MT*	*%Dist Adj MT*	*Stim Output PPC%*	*Stim Output FEF%*	*Stim Output IFG%*	*Cortical Dist M1*	*Cortical Dist PPC*	*Cortical Dist FEF*	*Cortical Dist IFG*	*PPC*	*FEF*	*IFG*
1	M	30	49	120	53	48	54	13.81	11.66	9.90	12.08	x	x	x
2	M	31	53	95	45	44	42	15.46	11.31	10.86	9.49	x	x	x
3	F	24	57	120	50	52	54	20.54	13.34	13.93	14.59	x	x	x
4	F	20	57	120	66	67	62	10.31	9.43	9.64	7.55	x	x	x
5	M	25	50	120	60	55	44	14.56	14.73	12.69	9.06	x	x	x
6	F	30	47	120	43	40	40	16.89	11.45	9.85	9.90	x	x	x
7	F	20	47	120	55	46	51	11.55	11.83	7.81	9.90	x	x	x
8	M	23	53	120	53	63	51	14.85	11.70	14.87	11.05	x	x	x
9	F	20	40	120	45	36	37	14.93	13.49	9.85	10.30			x
10	M	27	51	120	54	48	46	17.07	13.93	11.58	10.86	x	x	x
11	F	37	71	100	63	68	70	14.43	12.21	13.60	14.32	x	x	
12	F	20	62	120	65	61	51	17.05	14.35	13.08	9.70	x	x	x
13	M	31	51	117	44	50	46	17.67	11.45	13.89	12.53	x	x	x
14	M	25	46	105	49	45	54	14.34	14.49	12.88	16.43	x	x	x
15	M	28	62	115	49	48	46	18.44	12.08	11.79	11.45	x	x	x
16	M	23	56	90	50	40	41	19.20	18.79	14.35	14.87		x	
17	F	29	38	120	42	42	42	12.96	10.25	9.64	9.90	x	x	x
18	F	27	50	110	50	47	46	13.84	12.08	10.82	10.39	x	x	x
19	M	27	40	120	43	37	36	16.88	14.35	11.36	10.86	x	x	x
20	F	27	62	90	40	40	43	16.96	11.58	11.53	12.57		x	
21	M	27	45	120	55	51	50	11.50	11.79	10.00	9.80	x	x	x
M	*11M*	26.24	51.76	113.43	51.14	48.95	47.90	15.39	12.68	11.62	11.31	*n = 18*	*n = 20*	*n = 18*
SD		*4.40*	*8.26*	*10.67*	*7.60*	*9.32*	*8.14*	*2.62*	*2.00*	*1.91*	*2.22*			

Distances are expressed in millimeters.

APPENDIX B

Constraints to individual curve fitting:

Min(sub) = minimum Δ(adjRT) or minimum ΔSNARC data value between TMS = 0 msec and TMS = 367 msec or TMS = 333 msec for a given subject and number magnitude category (small vs. large)
Max(sub) = maximum Δ(adjRT) or minimum ΔSNARC data value between TMS = 0 msec and TMS = 367 msec or TMS = 333 msec for a given subject and number magnitude category (small vs. large)
$\min(\text{sub}) < y_1 < \max(\text{sub})$
$\min(\text{sub}) < y_2 < \max(\text{sub})$
$\min(\text{sub}) < a_1 < \max(\text{sub})$
$\min(\text{sub}) < a_2 < \max(\text{sub})$
$-200 < x_1 < 500$
$-200 < x_2 < 500$
$5 < b_1 < 200$
$5 < b_2 < 200$

APPENDIX C

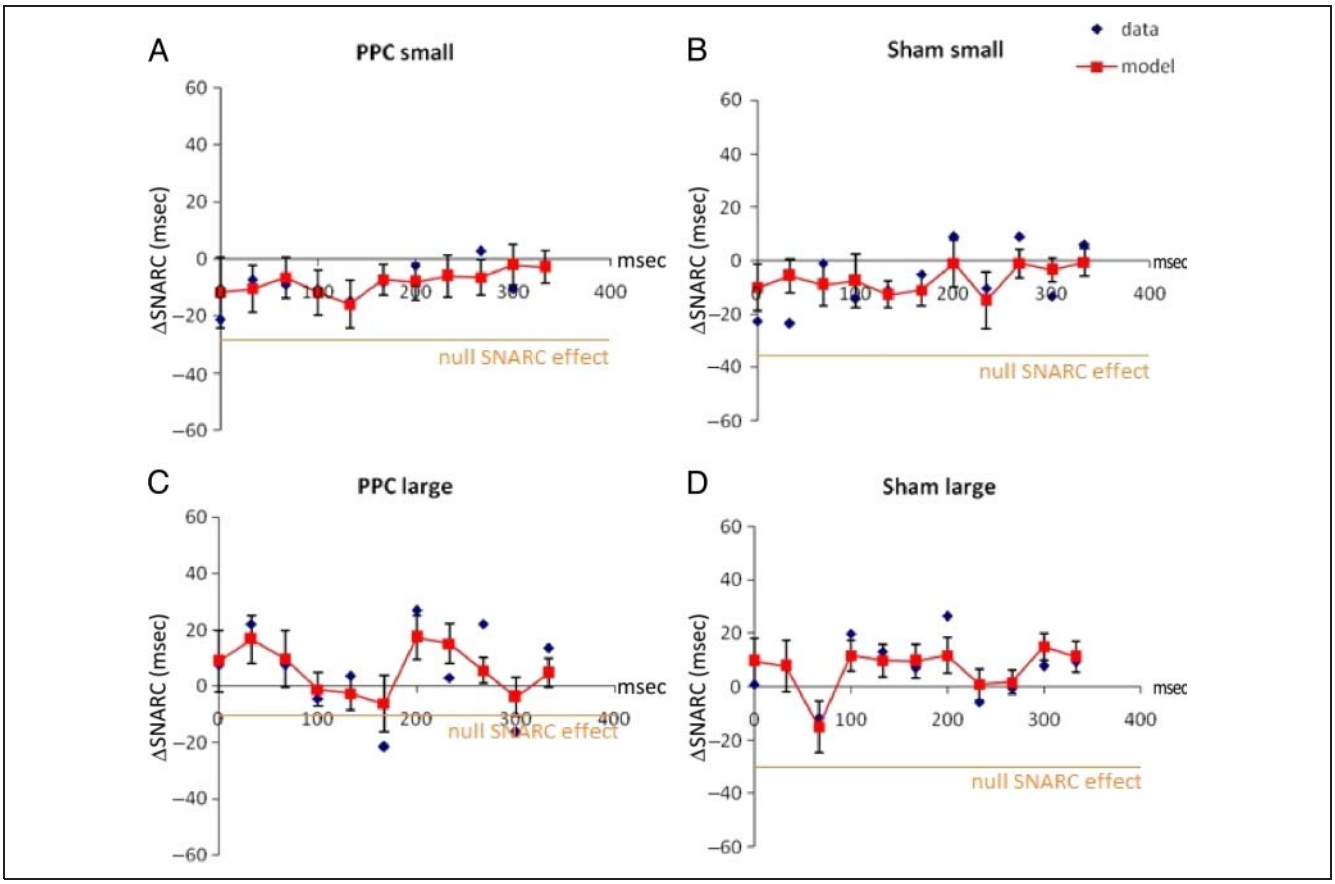

Group data and curve fits (vertical lines indicate standard error of the model's mean) are shown for rPPC (A and C) and sham (B and D), that is, for blocks where TMS did not significantly reduce or suppress the SNARC effect compared with the noTMS baseline (here corresponding to 0). Orange horizontal lines indicate the value of ΔSNARC, which would lead to a null SNARC effect.

APPENDIX D

Simple linear regressions were performed with either the amplitude of the earliest significant effect or its peak time as predictors (rIFG small; ΔSNARC = −43.7; *SEM* = 16.6; peak time: *M* = 26.3 msec; *SEM* = 8.9; see Table 1), and the amplitudes and peak times of effects of rFEF stimulation as dependent variables. Both peak time and amplitude of the rIFG effect on the SNARC for small numbers significantly predicted the peak time of the latest rFEF effect on the SNARC effect for small numbers (R^2 = .25, p = .04; and R^2 = .27, p = .03 respectively). In particular, a larger reduction of the SNARC effect with rIFG stimulation in the earlier phase predicted an earlier reduction of the SNARC effect because of TMS of rFEF in the later phase. However, an earlier reduction of the SNARC effect during rIFG TMS also predicted a later effect on rFEF, which suggests the presence of a tradeoff between amplitude and peak time for the early rIFG effect (i.e., the bigger the SNARC reduction, the higher its peak time; Pearson correlation approached significance: r = −.43, p = .08) and thus renders the result ambiguous. Neither peak time nor amplitude of the earlier rIFG effect showed a significant relation with either peak time or amplitude of the other rFEF effects (all ps > .21). Regressions on ΔSNARC were thus useful to localize a connection of potential interest. Figure 4A shows a graphical representation of the possible functional connection between the early effect of spTMS on rIFG and the later effect of spTMS on rFEF.

The ambiguity of these results highlights the necessity to consider that the SNARC reduction for small numbers is driven by slowing in the compatible condition with early rIFG stimulation and by facilitation in the incompatible condition with late rFEF stimulation, as shown in Nonlinear Regressions on ΔAdjRT for Compatible and Incompatible Trials section. To eliminate noise from the "ineffective" conditions and to identify the functional locus of the connection between rIFG and rFEF, we tested the relation between the early rIFG effect for the compatible condition and the following effect on rFEF for the incompatible condition only. This analysis is reported in main text, Linear Regression Analyses to Test for Potential rIFG-rFEF Functional Connectivity section.

APPENDIX E

Nonlinear Regression Analyses on ΔAdjRT Collapsed across Compatibility Conditions

The model accounted for 60–70% of the variance in each sub-condition of TMS site and number magnitude (small, large). Parameter specifications for all sites in the collapsed AdjRT analysis can be found in the table below, which shows that stimulation of all sites influenced performance, whereas no significant TMS effects were found in the sham condition. rFEF stimulation generally facilitated performance, and the effect reached significance for small numbers (peak time$_1$ = 68 msec; mean a_1 = −23 msec, p < .01 and peak time$_2$ = 222 msec; mean a_2 = −27.5 msec, p < .005). However, rFEF stimulation also reduced the SNARC effect for small numbers because of differential speeding on incompatible trials (see Nonlinear Regressions on ΔAdjRT for Compatible and Incompatible Trials section). These results, therefore, should be treated with caution. Stimulation of rIFG generally impaired performance. For small numbers, the significant early slowing (peak time$_1$ = 49 msec; mean a_1 = 37 msec, p < .005; see Figure 5C) corresponds to the modulation of the SNARC effect, which was reduced because of a differential slowing on compatible trials. For large numbers, rIFG stimulation also slowed performance both when applied early and also when applied at a later stage (peak time$_1$ = 28 msec; mean a_1 = 42 msec, p < .01 and peak time$_2$ = 219 msec;

Mean (*SEM*) Parameters Extracted from Double-Gaussian Regression Analyses of AdjRT (Collapsed across Response Compatibility)

				First Period			*Second Period*		
Site	*Magnitude*	R^2_{MEAN}	R^2_{TOTAL}	a_1	x_1	b_1	a_2	x_2	b_2
rFEF	Small	0.61	0.81	**−22.8 (7.4)****	67.8 (14.8)	37.4 (8.9)	**−27.5 (7.7)*****	221.6 (12.5)	29.3 (6)
	Large	0.61	0.72	−7.1 (10.1)	N/A	N/A	−5.1 (12.6)	N/A	N/A
rIFG	Small	0.68	0.91	**37.2*** (11.3)**	49 (9)	27.2 (6)	6.7 (9.5)	N/A	N/A
	Large	0.64	0.85	**41.7*** (10)**	28.3 (10.6)	45.6 (14.6)	**29.8*** (8.9)**	218.6 (12.8)	22.3 (4.2)
rPPC	Small	0.70	0.9	**44.8 (9.7)*****	61.5 (12.7)	25.1 (5.8)	−2.6 (8.4)	N/A	N/A
	Large	0.60	0.87	0.5 (11.2)	N/A	N/A	**−26.2 (6)*****	196.8 (15.2)	74.6 (15.2)
Sham	Small	0.65	0.84	9.9 (10.4)	N/A	N/A	3.4 (9.4)	N/A	N/A
	Large	0.63	0.77	6.2 (10.2)	N/A	N/A	11.6 (9.8)	N/A	N/A

Mean and total goodness of fit values are also provided for data modeling (R^2_{MEAN} and R^2_{TOTAL}, respectively). Significant key parameters (difference from zero) are indicated by asterisks. Note that peak times and bandwidths are interpretable only when the peak amplitude is also significant.

mean a_2 = 30 msec, $p < .005$; see Table 3 and Figure 5D). In this case, there was no concomitant modulation of SNARC and the TMS-induced impairments are therefore not as ambiguous as the effect for small numbers. Clear and opposing effects of rPPC stimulation were observed for small versus large numbers. For small numbers, significant interference from TMS was found in the initial phase, peaking at +61 msec (a_1 = 44.8 msec, $p < .005$; Figure 5A). For large numbers, on the contrary, significant TMS-induced facilitation was observed in the second phase, peaking at +197 msec (mean baseline-corrected a_2 = −26.2 msec, $p < .005$).

Reprint requests should be sent to Dr. Elena Rusconi, Department of Neurosciences, Section of Physiology, University of Parma, Via Volturno 39/E, I-43100 Parma, Italy, or via e-mail: elena.rusconi@gmail.com.

REFERENCES

Ansari, D. (2008). Effects of development and enculturation on number representation in the brain. *Nature Reviews Neuroscience, 9,* 278–291.

Barash, S. (2003). Paradoxical activities: Insight into the relationship of parietal and prefrontal cortices. *Trends in Neuroscience, 26,* 582–589.

Bardi, L., Kanai, R., Mapelli, D., & Walsh, V. (2012). TMS of the FEF interferes with spatial conflict. *Journal of Cognitive Neuroscience, 24,* 1305–1313.

Bisiach, E., & Luzzatti, C. (1978). Unilateral neglect of representational space. *Cortex, 14,* 129–133.

Brighina, F., Bisiach, E., Oliveri, M., Piazza, A., La Bua, V., Daniele, O., et al. (2003). 1-Hz repetitive transcranial magnetic stimulation of the unaffected hemisphere ameliorates contralesional visuospatial neglect in humans. *Neuroscience Letters, 336,* 131–133.

Butterworth, B. (2010). Foundational numerical capacities and the origins of dyscalculia. *Trends in Cognitive Sciences, 14,* 534–541.

Cattaneo, Z., Silvanto, J., Battelli, L., & Pascual-Leone, A. (2009). The mental number line modulates visual cortical excitability. *Neuroscience Letters, 462,* 253–256.

Cattaneo, Z., Silvanto, J., Pascual-Leone, A., & Battelli, L. (2009). The role of the angular gyrus in the modulation of visuospatial attention by the mental number line. *Neuroimage, 44,* 563–568.

Chambers, C. D. C., Allen, C. P. G., Maizey, L., & Williams, M. A. (in press). Is delayed foveal feedback critical for extrafoveal perception? *Cortex*.

Chambers, C. D., & Mattingley, J. B. (2005). Neurodisruption of selective attention: Insights and implications. *Trends in Cognitive Sciences, 9,* 542–550.

Chambers, C. D., Payne, J. M., Stokes, M. G., & Mattingley, J. B. (2004). Fast and slow parietal pathways mediate spatial attention. *Nature Neuroscience, 7,* 217–218.

Corbetta, M., Patel, G., & Shulman, G. L. (2008). The reorienting system of the human brain: From environment to theory of mind. *Neuron, 58,* 306–324.

Corbetta, M., & Shulman, G. L. (2002). Control of goal-directed and stimulus-driven attention in the brain. *Nature Reviews Neuroscience, 3,* 201–215.

Corbetta, M., & Shulman, G. L. (2011). Spatial neglect and attention networks. *Annual Reviews Neuroscience, 34,* 569–599.

de Hevia, M. D., Vallar, G., & Girelli, L. (2008). Visualizing numbers in the mind's eye: The role of visuo-spatial processes in numerical abilities. *Neuroscience and Biobehavioral Reviews, 32,* 1361–1372.

Dehaene, S., Bossini, S., & Giraux, P. (1993). The mental representation of parity and number magnitude. *Journal of Experimental Psychology: General, 122,* 371–396.

Dehaene, S., Piazza, M., Pinel, P., & Cohen, L. (2003). Three parietal circuits for number processing. *Cognitive Neuropsychology, 20,* 487–506.

Desimone, R., & Duncan, J. (1995). Neural mechanisms of selective visual attention. *Annual Review of Neuroscience, 18,* 193–222.

Doricchi, F., Guariglia, P., Gasparini, M., & Tomaiuolo, F. (2005). Dissociation between physical and mental number line bisection in right hemisphere damage. *Nature Neuroscience, 8,* 1663–1665.

Duncan, J., Humphreys, G., & Ward, R. (1997). Competitive brain activity in visual attention. *Current Opinion in Neurobiology, 7,* 255–261.

Fias, W., & Fischer, M. H. (2005). Spatial representation of number. In J. I. D. Campbell (Ed.), *Handbook of mathematical cognition* (pp. 43–54). New York: Psychology Press.

Fischer, M. H. (2006). The future for SNARC could be stark. *Cortex, 42,* 1066–1068.

Fitousi, D., Shaki, S., & Algom, D. (2009). The role of parity, physical size, and magnitude in numerical cognition: The SNARC effect revisited. *Attention, Perception and Psychophysics, 71,* 143–155.

Fox, M. D., Corbetta, M., Snyder, A. Z., Vincent, J. L., & Raichle, M. E. (2006). Spontaneous neuronal activity distinguishes human dorsal and ventral attention systems. *Proceedings of the National Academy of Sciences, U.S.A., 103,* 10046–10051.

Galfano, G., Rusconi, E., & Umiltà, C. (2006). Number magnitude orients attention, but not against one's will. *Psychonomic Bulletin and Review, 13,* 869–874.

Gevers, W., Santens, S., Dhooge, E., Chen, Q., Van den Bossche, L., Fias, W., et al. (2010). Verbal-spatial and visuospatial coding of number-space interactions. *Journal of Experimental Psychology: General, 139,* 180–190.

Gevers, W., Verguts, T., Reynvoet, B., Caessens, B., & Fias, W. (2006). Numbers and space: A computational model of the SNARC effect. *Journal of Experimental Psychology: Human Perception and Performance, 32,* 32–44.

Göbel, S. M., Calabria, M., Farnè, A., & Rossetti, Y. (2006). Parietal rTMS distorts the mental number line: Simulating "spatial" neglect in healthy subjects. *Neuropsychologia, 44,* 860–868.

Göbel, S. M., Walsh, V., & Rushworth, M. F. (2001). The mental number line and the human angular gyrus. *Neuroimage, 14,* 1278–1289.

Grosbras, M. H., & Paus, T. (2002). Transcranial magnetic stimulation of the human frontal eye field: Effects on visual perception and attention. *Journal of Cognitive Neuroscience, 18,* 3121–3126.

Heinen, K., Ruff, C. C., Bjoertomt, O., Schenkluhn, B., Bestmann, S., Blankenburg, F., et al. (2011). Concurrent TMS-fMRI reveals dynamic interhemispheric influences of right parietal cortex during exogenously cued visuospatial attention. *European Journal of Neuroscience, 33,* 991–1000.

Hilgetag, C., Théoret, H., & Pascual-Leone, A. (2001). Enhanced visuospatial attention ipsilateral to rTMS-induced "virtual lesions" of human parietal cortex. *Nature Neuroscience, 4,* 953–957.

Hubbard, E. M., Piazza, M., Pinel, P., & Dehaene, S. (2005). Interactions between number and space in parietal cortex. *Nature Reviews Neuroscience, 6,* 435–448.

Husain, M., & Rorden, C. (2003). Non-spatially lateralized mechanisms in hemispatial neglect. *Nature Reviews Neuroscience, 4,* 26–36.

Juan, C.-H., Campana, G., & Walsh, V. (2004). Cortical interactions in vision and awareness: Hierarchy in reverse. *Progress in Brain Research, 144,* 117–130.
Juan, C.-H., Muggleton, N. G., Tzeng, O. J., Hung, D. L., Cowey, A., & Walsh, V. (2008). Segregation of visual selection and saccades in human frontal eye fields. *Cerebral Cortex, 18,* 2410–2415.
Kastner, S., & Ungerleider, L. (2000). Mechanisms of visual attention in the human cortex. *Annual Review of Neuroscience, 23,* 315–341.
Khayat, P. S., Pooresmaeili, A., & Roelfsema, P. R. (2009). Time course of attentional modulation in the frontal eye field during curve tracing. *Journal of Neurophysiology, 101,* 1813–1822.
Khayat, P. S., Spekreijse, H., & Roelfsema, P. R. (2006). Attention lights up new object representations before the old ones fade away. *Journal of Neuroscience, 26,* 138–142.
Kornblum, S., Hasbroucq, T., & Osman, A. (1990). Dimensional overlap: Cognitive basis for stimulus–response compatibility. A model and taxonomy. *Psychological Review, 97,* 253–270.
Kosslyn, S., Ganis, G., & Thompson, W. (2001). Neural foundations of imagery. *Nature Reviews Neuroscience, 2,* 635–642.
Kosslyn, S., Pascual-Leone, A., Felician, O., Camposano, S., Keenan, J. P., Thompson, W. L., et al. (1999). The role of area 17 in visual imagery: Convergent evidence from PET and rTMS. *Science, 284,* 167–170.
Lorch, R., & Myers, J. (1990). Regression analyses of repeated-measures data in cognitive research. *Journal of Experimental Psychology: Learning, Memory, and Cognition, 16,* 149–157.
Mapelli, D., Rusconi, E., & Umiltà, C. (2003). The SNARC effect: An instance of the Simon effect? *Cognition, 88,* B1–B10.
Muggleton, N. G., Juan, C. H., Cowey, A., & Walsh, V. (2003). Human frontal eye fields and visual search. *Journal of Neurophysiology, 89,* 3340–3343.
Nieder, A., & Dehaene, S. (2009). Representation of number in the brain. *Annual Reviews Neuroscience, 32,* 185–208.
Nieder, A., & Miller, E. K. (2004). A parieto-frontal network for visual numerical information in the monkey. *Proceedings of the National Academy of Sciences, U.S.A., 101,* 7457–7462.
Oliveri, M., Rausei, V., Koch, G., Torriero, S., Turriziani, P., & Caltagirone, C. (2004). Overestimation of numerical distances in the left side of space. *Neurology, 63,* 2139–2141.
O'Shea, J., Muggleton, N. G., Cowey, A., & Walsh, V. (2004). Timing of target discrimination in human frontal eye fields. *Journal of Cognitive Neuroscience, 16,* 1060–1067.
Rao, S. C., Rainer, G., & Miller, E. K. (1997). Integration of what and where in the primate prefrontal cortex. *Science, 276,* 821–824.
Riello, M., & Rusconi, E. (2011). Unimanual SNARC effect: Hand matters. *Frontiers in Psychology, 2,* 372.
Rizzuto, D. S., Mamelak, A. N., Sutherling, W. W., Fineman, I., & Andersen, R. A. (2005). Spatial selectivity in human ventrolateral prefrontal cortex. *Nature Neuroscience, 8,* 415–417.
Rosenthal, R. (1991). *Meta-analytic procedures for social research* (2nd ed.). Newbury Park, CA: Sage.
Rusconi, E., Bueti, D., Walsh, V., & Butterworth, B. (2011). Contribution of frontal cortex to the spatial representation of number. *Cortex, 47,* 2–13.
Rusconi, E., Turatto, M., & Umiltà, C. (2007). Two orienting mechanisms in posterior parietal lobule: An rTMS study of the Simon and SNARC effects. *Cognitive Neuropsychology, 24,* 373–392.
Rusconi, E., Walsh, V., & Butterworth, B. (2005). Dexterity with numbers: rTMS overleft angular gyrus disrupts finger gnosis and number processing. *Neuropsychologia, 43,* 1609–1624.
Salillas-Pérez, E. S., Basso, D., Baldi, M., Semenza, C., & Vecchi, T. (2009). Motion on numbers: Transcranial magnetic stimulation on the ventral intraparietal sulcus alters both numerical and motion processes. *Journal of Cognitive Neuroscience, 21,* 2129–2138.
Sandrini, M., & Rusconi, E. (2009). A brain for numbers. *Cortex, 45,* 796–803.
Sandrini, M., Umiltà, C., & Rusconi, E. (2011). The use of transcranial magnetic stimulation in cognitive neuroscience: A new synthesis of methodological issues. *Neuroscience and Biobehavioral Reviews, 35,* 516–536.
Santens, S., & Gevers, W. (2008). The SNARC effect does not imply a mental number line. *Cognition, 108,* 263–270.
Sato, M., Cattaneo, L., Rizzolatti, G., & Gallese, V. (2007). Numbers within our hands: Modulation of corticospinal excitability of hand muscles during numerical judgment. *Journal of Cognitive Neuroscience, 19,* 684–693.
Shulman, G. L., Astafiev, S. V., Franke, D., Pope, D. L., Snyder, A. Z., McAvoy, M. P., et al. (2009). Interaction of stimulus-driven reorienting and expectation in ventral and dorsal frontoparietal and basal ganglia-cortical networks. *Journal of Neuroscience, 29,* 4392–4407.
Simon, O., Mangin, J. F., Cohen, L., Le Bihan, D., & Dehaene, S. (2002). Topographical layout of hand, eye, calculation, and language-related areas in the human parietal lobe. *Neuron, 33,* 475–487.
Stevens, L. K., McGraw, P. V., Ledgeway, T., & Schluppeck, D. (2009). Temporal characteristics of global motion processing revealed by transcranial magnetic stimulation. *European Journal of Neuroscience, 30,* 2415–2426.
Stokes, M. G., Chambers, C. D., Gould, I. C., English, T., McNaught, E., McDonald, O., et al. (2007). Distance-adjusted motor threshold for transcranial magnetic stimulation. *Clinical Neurophysiology, 118,* 1617–1625.
Stokes, M. G., Chambers, C. D., Gould, I. C., Henderson, T. R., Janko, N. E., Allen, N. B., et al. (2005). Simple metric for scaling motor threshold based on scalp–cortex distance: Application to studies using transcranial magnetic stimulation. *Journal of Neurophysiology, 94,* 4520–4527.
Sylvester, C. M., Shulman, G. L., Jack, A. I., & Corbetta, M. (2007). Asymmetry of anticipatory activity in visual cortex predicts the locus of attention and perception. *Journal of Neuroscience, 27,* 14424–14433.
Townsend, J. T., & Ashby, F. G. (1983). *Stochastic modelling of elementary psychological processes*. London: Cambridge University Press.
Umarova, R. M., Saur, D., Schnell, S., Kaller, C. P., Vry, M. S., Glauche, V., et al. (2010). Structural connectivity for visuospatial attention: Significance of ventral pathways. *Cerebral Cortex, 20,* 121–129.
Umiltà, C., Priftis, K., & Zorzi, M. (2009). The spatial representation of numbers: Evidence from neglect and pseudoneglect. *Experimental Brain Research, 192,* 561–569.
Walsh, V. (2003). A theory of magnitude: Common cortical metrics of time, space and quantity. *Trends in Cognitive Sciences, 7,* 483–488.
Wood, G., Willmes, K., Nuerk, H. C., & Fischer, M. H. (2008). On the cognitive link between space and number: A meta-analysis of the SNARC effect. *Psychology Science Quarterly, 50,* 489–525.
Zorzi, M., Priftis, K., & Umiltà, C. (2002). Brain damage: Neglect disrupts the mental number line. *Nature, 417,* 138–139.
Zorzi, M., & Umiltà, C. (1995). A computational model of the Simon effect. *Psychological Research, 58,* 193–205.